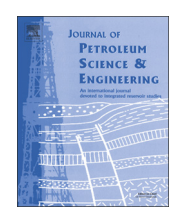


Contents lists available at ScienceDirect

# Journal of Petroleum Science and Engineering

journal homepage: www.elsevier.com/locate/petrol



# A novel multi-hybrid model for estimating optimal viscosity correlations of Iranian crude oil



Bahram Ghorbani <sup>a,\*</sup>, Mohsen Hamedi <sup>a</sup>, Reza Shirmohammadi <sup>b</sup>, Mehdi Mehrpooya <sup>c</sup>, Mohammad-Hossein Hamedi <sup>a</sup>

- <sup>a</sup> Mechanical Engineering Faculty, Energy Conversion Group KNToosi University of technology, Tehran, Iran
- <sup>b</sup> Young Researchers and Elite Club, South Tehran Branch, Islamic Azad University, Tehran, Iran
- <sup>c</sup> Renewable Energies and Environmental Department, Faculty of New Science and Technologies, University of Tehran, Tehran, Iran

#### ARTICLE INFO

Article history:
Received 3 June 2015
Received in revised form
24 September 2015
Accepted 29 January 2016
Available online 1 February 2016

Keywords:
Oil viscosity
Correlation coefficient
GMDH algorithm
Genetic algorithm

#### ABSTRACT

Viscosity is defined as one of the principal measure of fluid resistance to shear stress. Efficiently estimating and predicting of oil viscosity in different operating conditions is vital. A new multi-hybrid model is employed to estimate the crude oil viscosity below, at, and above the bubble points using the South Pars data located in Persian Gulf. Five variables consisting oil API gravity, reservoir temperature, solution gas—oil ratio, pressure and saturation pressure as inputs are imposed to the model. A general structure of group method of data handling along with Genetic algorithm, are proposed to obtain efficient polynomial correlations to estimate oil viscosity at the aforementioned points. These correlations also are compared with seven correlations presented in previous studies. Results show that the proposed multi-hybrid model is superior to the other models for estimating the viscosity values of Iranian crude oils.

© 2016 Elsevier B.V. All rights reserved.

Nomenclatures	S n	Standard deviation Number of data points
E <sub>i</sub> Percent relative error E <sub>a</sub> Percent mean absolute relative error E <sub>r</sub> Percent mean relative error	or $egin{array}{c} r \\ ar{X} \\ i \end{array}$	Correlation coefficient Mean value Observation index

Shirmohammadi et al. (2015) employed a hybrid group method of data handling (GMDH) along with linking between Aspen HY-SYS and MATLAB software, optimized with Genetic algorithm (GA), to obtain efficient polynomial correlation to estimate optimal consumed power for two cascade refrigeration cycles.

Ghorbani et al. (2014) proposed a GMDH artificial neural network, optimized with genetic algorithm (GA), to obtain efficient polynomial correlation to forecast oil viscosity. The obtained correlations were compared with previous research correlations using the large set of Iranian oil data. They also provided a comprehensive computational and statistical result to assess the performance of the proposed methods. Results illustrated the hybrid model had very good behavior for estimating the viscosity of crude oils.

Hemmati-Sarapardeh et al. (2013) evaluated the most frequently used oil viscosity correlations using a large databank of Iranian oil reservoirs. They recommended three of the most accurate correlations for each region, comprising dead oil viscosity, viscosity below bubble point, viscosity at bubble point and the under saturated oil viscosity, for Iranian oil reservoirs. Ultimately, they developed four correlations for Iranian oil reservoirs which have simplified functional format.

Hou et al. (2015) presented a model for Shanbei crude oil blending to improve the total yield of fractions and reduce the viscosity of the mixed crude oils.

Recently, many scholars employed the artificial neural network to predict oil viscosity (Al-Marhoun et al., 2012; Ardalan et al., 2009; Ghaderi, 2012; Makinde et al., 2012; Torabi et al., 2011). Abedini (2010) also developed an empirical formula to forecast oil viscosity. They also validated sensitivity analysis of viscosity by diverse graphs. A correlation method for forecasting crude oil viscosities was examined by Naseri et al. (2005).

Hajizadeh (2007a, 2007b) applied genetic algorithm techniques for predicting reservoir fluid viscosity. An impact analysis was performed on the input parameters, which are pressure, temperature, gas-oil ratio, and oil density, indicating that the temperature has the greatest impact on the reservoir fluid viscosity followed by oil density, pressure and gas-oil ratio. The genetic algorithm indicated prediction of viscosity with a good accuracy for testing data.

In this study, five input variables consist of oil API gravity (API), pressure (P), saturation pressure (P<sub>b</sub>), solution gas–oil ratio (R<sub>s</sub>), reservoir temperature (T<sub>f</sub>) are imposed to the present multi-hybrid model. The purpose of this paper is to obtain a relationship between oil viscosity at reservoir pressure, temperature, and other parameters of crude oil. The relationship can easily be achieved with PVT analysis. This relation is studied in three different cases of pressure at the bubble point, below the bubble point, and above the bubble point pressure. The present model can obtain efficient polynomial correlation to estimate oil viscosity at the aforementioned points.

#### 2. GMDH neural networks

The GMDH algorithms can be applied in a great variety of areas for anticipating as well as systems modeling and optimization. The GMDH algorithm can also be considered from two different facets, mathematical basis as well as modeling theory and analysis of the system. Mathematically, the GMDH algorithm is embedded in

analyzing Volterra function series to a quadratic two-variable polynomial. Volterra series is converted into a set of chain recursive equations in this analysis. The algebraic substitution of each recursive relation then can results in the re-establishment of Volterra series. A mathematical model can be characterized as a set of neuron. Dissimilar pairs in each layer are linked by a quadratic polynomial to produce new neurons in the next layer. Identification problem can be defined to find a function  $\hat{f}$  that can forecast output  $\hat{y}$  for an assumed input vector  $X = (x_1, x_2, x_3, ..., x_n)$ . The definite output can be defined as follows: (Nariman-Zadeh et al., 2003; Nariman-Zadeh et al., 2005)

$$y_i = f(x_{i1}, x_{i2}, x_{i3}, ..., x_{in})$$
 (i = 1, 2, 3, ... M)

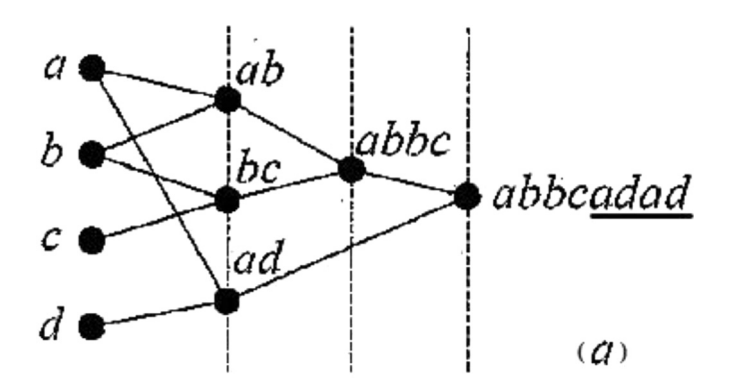
GMDH is then trained by assumed input vector  $X = (x_{i1}, x_{i2}, x_{i3}, ..., x_{in})$  to forecast the output values  $\hat{f}_i$  as follows:

$$\hat{y}_i = \hat{f}(x_{i1}, x_{i2}, x_{i3}, \dots, x_{in}) \quad (i = 1, 2, 3, \dots M)$$
(2)

The squared difference between the definite and anticipated output can be minimized as:

$$\sum_{i=1}^{M} \left[ \hat{f}(x_{i1}, x_{i2}, x_{i3}, \dots, x_{in}) - y_i \right]^2 \to \min$$
(3)

An intricate discrete form of the Volterra series is employed to make a general connection between input and output variables:



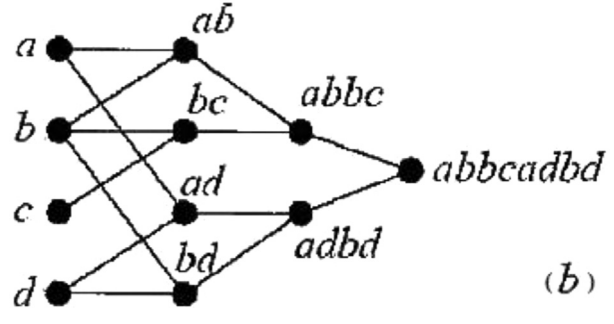


**Fig. 1.** Network structure of a chromosome (Shirmohammadi et al., 2015). (a) GS-GMDH type, (b) CS-GMDH type.

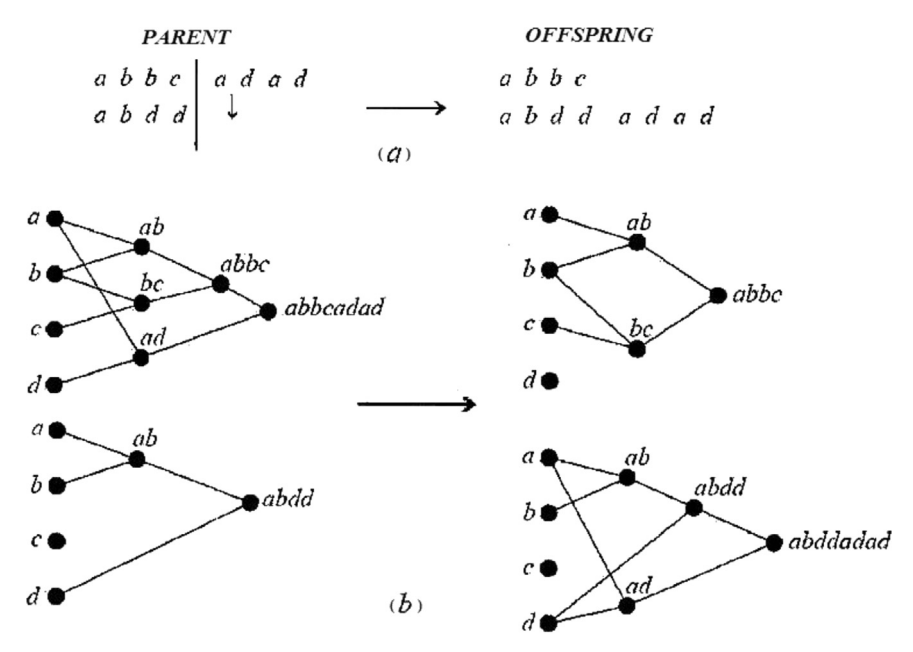


Fig. 2. Crossover operation Shirmohammadi et al. (2015). (a) For two individuals in GS-GMDH networks, (b) on two GS-GMDH networks.

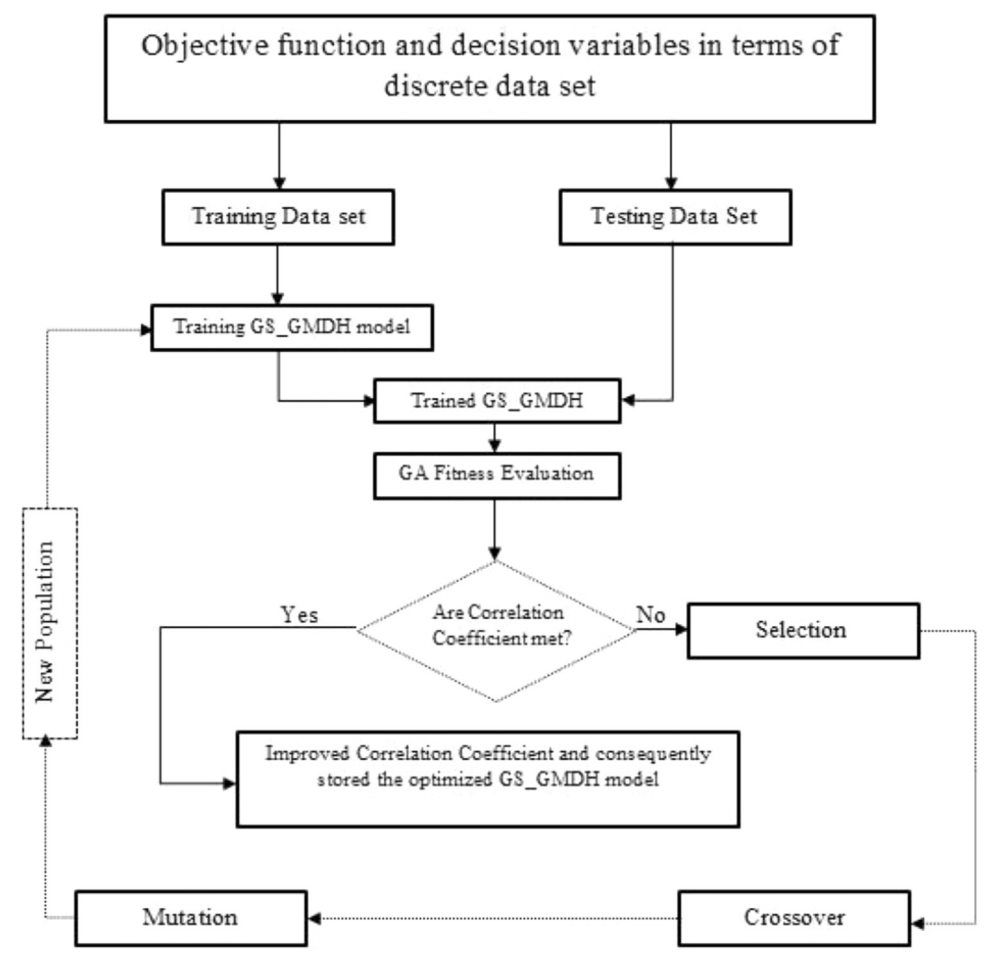


Fig. 3. Procedure of parameters tuning by combination of GS-GMDH and GA algorithms.

**Table 1**Tuning parameters in the Genetic algorithm for viscosity below, at, and above the bubble points.

Tuning parameters in the Genetic Algorithm for viscosity values				
Tuning parameters	Below	At	Above	
Population size	365	57	287	
Maximum number of generations	1095	171	861	
Probability of crossover	70%	70%	70%	
Probability of mutation	1%	1%	1%	
Number of crossover point	2	2	2	

$$y = a_{\circ} + \sum_{i=1}^{n} a_{i}x_{i} + \sum_{i=1}^{n} \sum_{j=1}^{n} a_{ij}x_{i}x_{j} + \sum_{i=1}^{n} \sum_{j=1}^{n} \sum_{k=1}^{n} a_{ijk}x_{i}x_{j}x_{k} + \dots$$
(4)

The above mathematical depiction can be expressed by a partial quadratic polynomials system comprising two variables as follows:

$$\hat{\hat{y}} = G(x_i, x_i) = a_\circ + a_1 x_i + a_2 x_i + a_3 x_i^2 + a_4 x_i^2 + a_5 x_i x_i$$
 (5)

The above-mentioned system is recursively employed to create the general mathematical connection between input and output variables by connected neurons. Regression techniques are employed to calculate  $a_i$  value in Eq. (5). The difference between actual and calculated output variables can be minimized in terms of input variables.

The following equations are acquired for each row of M data triples using the quadratic sub-expression in the Eq. (5).

$$Aa = Y \tag{6}$$

$$a = \{ a_{\circ}, a_{1}, a_{2}, a_{3}, a_{4}, a_{5} \}$$
 (7)

$$Y = \{y_1, y_2, y_3, \dots y_M\}^T$$
 (8)

where Y is the vector of output values, and a is the vector of unknown coefficients for the quadratic polynomial in Eq. (5).

$$a = \left(A^T A\right)^{-1} A^T Y \tag{11}$$

Eq. (11) also defines the best quadratic coefficient vector for the entire set of M data triples. This process is reiterated in the next hidden layer for each of the neuron with respect to the network connectivity topology.

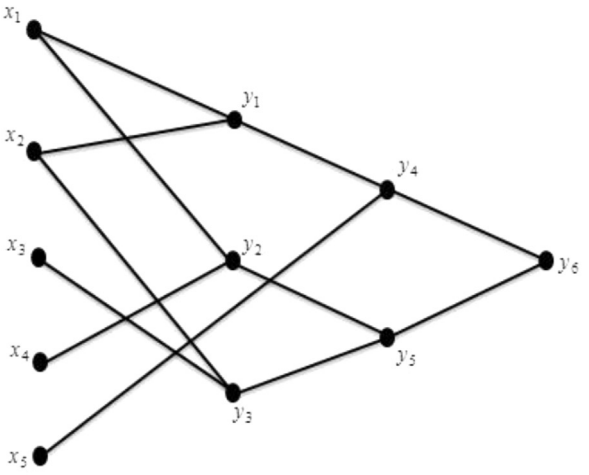
In the second part, the GMDH algorithms are based on the modeling theory and analysis of systems. The GMDH neural network is a self-organizing, unidirectional structure with multiple layers. These layers are composed of several neurons, which have an analogous structure. (Nariman-Zadeh et al., 2003).

Singular Value Decomposition (SVD) also is employed to design of such GMDH-type networks. SVD is a method for solving most linear least squares problems that some singularities might exist in the normal equations. The most popular technique for computing the SVD was proposed in (Shirmohammadi et al., 2015).

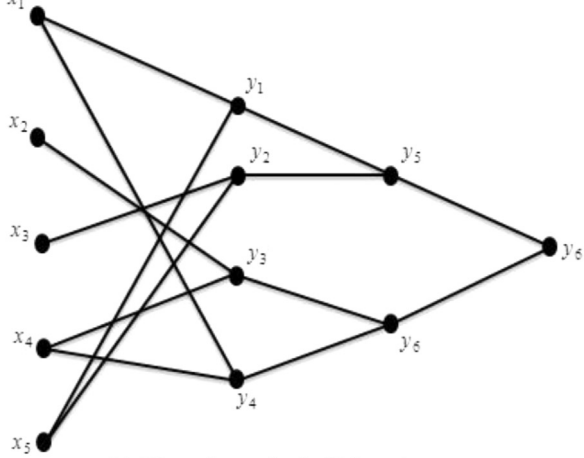
## $2.1. \ \ Topology \ design \ of \ GMDH-type \ ANNs \ using \ genetic \ algorithm$

Genetic algorithms as an evolutionary algorithm is widely applied for different features of design in neural networks because of their unique capabilities of finding a global optimum in multimodal and/or non-differentiable search space (Ardalan et al., 2009; Nariman-Zadeh et al., 2003; Shirmohammadi et al., 2015).

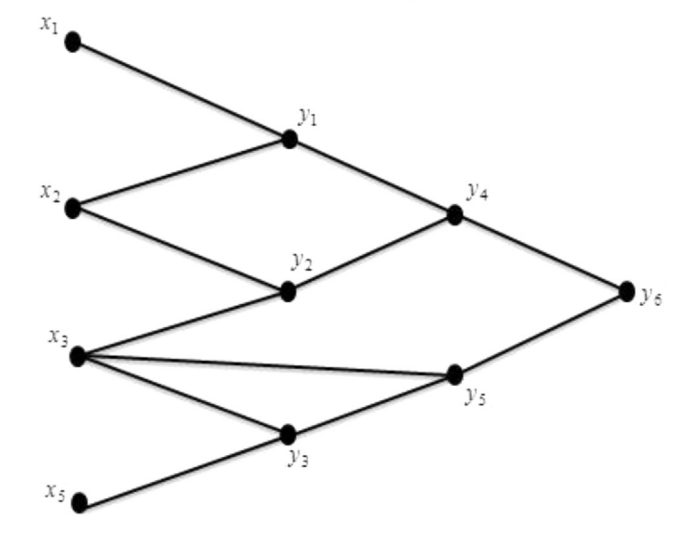
GMDH artificial neural networks can be divided into the two types consisting of GS-GMDH and CS-GMDH neural networks. In the GS-GMDH neural networks, neurons connections can occur between different layers, which are not necessarily adjacent ones (Fig.1 (a)).



a) Viscosity below the bubble point



b) Viscosity at the bubble point



### c) Viscosity above the bubble point

**Fig. 4.** Evolved structure of GS-GMDH neural network for. (a) Viscosity below the bubble point. (b) Viscosity at the bubble point. (c) Viscosity above the bubble point.

Whereas, in the CS-GMDH neural networks such connections occur only between adjacent layer (Fig. 1(b)) (Nariman-Zadeh et al., 2003; Shirmohammadi et al., 2015).

According to Fig. 2(a) and (b), the crossover process can alter the building blocks information of such GS-GMDH neural networks. In this

 Table 2

 Experimental data range for saturated and under-saturated reservoir oil viscosity.

Oil properties	Under-saturated	Saturated
Oil API gravity	21.55-30.62	21.55-37.62
Reservoir temperature (F)	100-250	100-250
Solution gas-oil ratio (scf/stb)	302-1601	302-1601
Saturation pressure (psia)	773-5931	773-5931
Pressure (psia)	110-4790	110-4790
Saturated viscosity (cP)	0.32-6.23	0.27-4.12

way, the two types of GS-GMDH and CS-GMDH neural networks can be transformed to each other, depicted in Fig. 2(b). Mutation process can also convert a GS-GMDH neural network to a CS-GMDH one or vice versa. (Madandoust et al., 2010; Nariman-Zadeh et al., 2003; Shirmohammadi et al., 2015)

#### 3. Presented multi-hybrid model

Overall assessment and training of the developed correlations are carried out by a set of Iranian oil data. This sample have over 600 valid data points, measured in the laboratory, and is divided into two general categories of saturated and under-saturated oil. In presented multi-hybrid model in Fig. 3, the correlation of each datasets is obtained from training datasets. These correlations are then tested by the testing datasets, which are never observed throughout the training. About 90% of each data set is applied for training in order to derive a GS-GMDH algorithm, and the rest is used for validating the correlation. The best value that can be gained for the variable is equal to 1. If the appropriate value of correlation, which is more than 0.95, is not obtained, Genetic algorithm according to range of decision variables would generate new data stochastically and the new data

then enter to the GS-GMDH model. Again these data herein are employed to obtain new appropriate correlation. This step is being continued to obtain the appropriate correlation. Tuning parameters of Genetic algorithm, used in this study, are given in Table 1.

#### 4. Modeling of viscosity correlation

In this paper, five input variables and an output variable are employed for modeling of viscosity below, at and above the bubble point using GS-GMDH neural networks. The five variables are recognized as primary input data (pressure  $x_1$ ; reservoir temperature,  $x_2$ :  $T_f$ ; solution gas-oil ratio,  $x_3$ :  $R_s$ ; saturation pressure,  $x_4$ :  $P_b$ ; oil API gravity,  $x_5$ :  $\frac{141.5}{131.5 + API}$ ) and an output data  $y_6$  representing viscosity at the aforementioned points. The total number of available data for training and testing the correlation viscosity below, at and above the bubble point are 365, 287, and 57, respectively. These datasets are divided into training and testing sets to validate the forecast aptitude of the GS-GMDH neural networks. The training sets, consisting of 295 out of 365 data, 51 out of 57, and 199 out of 287 are employed for training and. The rest of unanticipated data, which are testing set, are just employed for testing to indicate the forecast aptitude of the evolved GS-GMDH neural network model throughout the training process. The structure of these GS-GMDH models are illustrated in Fig. 4 corresponding to the genome representations of  $y_6$  for viscosity above, at, and below of the bubble points.

#### 5. Correlations development

The PVT experimental data sample for South pars crude oils located in Persian gulf is measured. The samples are tested

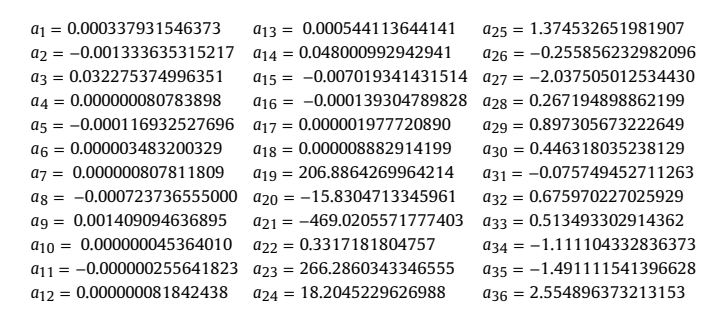
**Table 3**Accuracy of viscosity correlations for prediction of saturated oil and under-saturated oil viscosities.

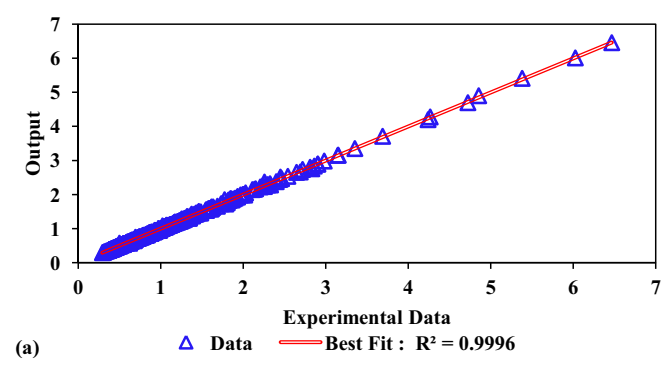
Saturated oil viscosity					
Viscosity at the bubble point	Correlation	MAE	ME	S	R
	The present research	0.01058	0.0000104	0.8295	0.999786
	Ghorbani et al. (2014)	12.48	-3.34	18.24	0.97
	Elsharkawy and Alikhan (1999)	22.9413	-20.4634	20.1123	0.9245
	Khan et al. (1987)	23.52	-6.34	31.12	0.78
	Labedi (1992)	52.05	-52.05	31.40	0.46
	Kartoatmodjo and Schmidt (1994)	32.45	17.44	34.88	086
	Petrosky and Farshad (1995)	81.98	-80.72	44.65	0.59
	Naseri et al. (2005)	17.4	- 13.42	22.17	0.84
Viscosity below the bubble point	The present research	3.77	0.0018	0.6731	0.998
3	Ghorbani et al. (2014)	13.57	-3.15	17.49	0.96
	Elsharkawy and Alikhan (1999)	25.60	19.77	24.10	0.74
	Khan et al. (1987)	32.01	-21.77	38.29	0.57
	Labedi (1992)	43.68	-42.16	30.66	0.42
	Kartoatmodjo and Schmidt (1994)	48.13	44.88	28.97	061
	Petrosky and Farshad (1995)	63.01	-58.24	53.54	0.65
	Naseri et al. (2005)	31.13	-0.28	24.15	0.76
Under-saturated oil viscosity					
Viscosity above the bubble point	Correlation	MAE	ME	S	R
	The present research	0.268	0.000012	0.835	0.99998
	Ghorbani et al. (2014)	10.95	-1.88	13.95	0.98
	Elsharkawy and Alikhan (1999)	25.60	19.77	24.10	0.74
	Khan et al. (1987)	21.54	-5.06	29.46	0.79
	Labedi (1992)	69.13	-69.13	77.83	0.44
	Kartoatmodjo and Schmidt (1994)	31.29	14.81	36.31	0.84
	Petrosky and Farshad (1995)	77.79	-76.09	45.33	0.63
	Naseri et al. (2005)	22.18	- 12.16	26.1	0.86

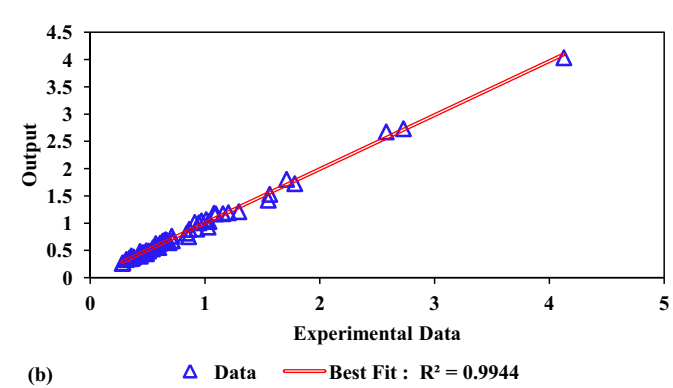
meticulously and the values of the parameters and oil viscosity are derived. Details of these data are presented in Table 2.

Corresponding polynomial representation of the model for below, at, and above the bubble points are drown as follows.

#### 5.1. Correlation A (viscosity below the bubble point)







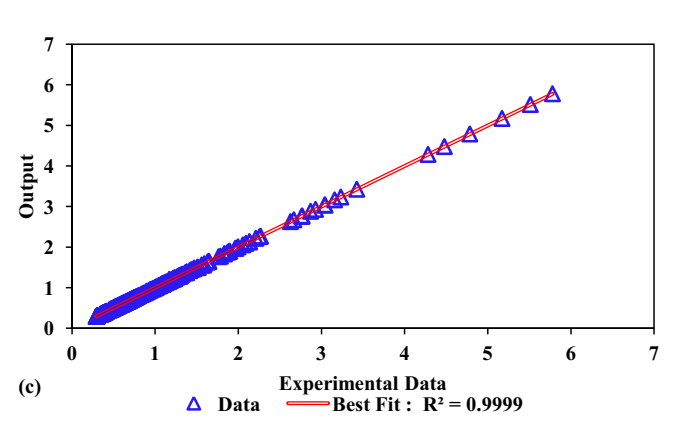


**Fig. 5.** Scatter diagram based on presented approach in terms of correlation coefficient  $(R^2)$ . (a) Viscosity below the bubble point. (b) Viscosity at the bubble point. (c) Viscosity above the bubble point.

$$y_{1} = a_{1} + (a_{2}x_{1}) + (a_{3}x_{2}) + (a_{4}x_{1}^{2}) + (a_{5}x_{2}^{2}) + (a_{6}x_{1}x_{2})$$

$$y_{2} = a_{7} + (a_{8}x_{1}) + (a_{9}x_{4}) + (a_{10}x_{1}^{2}) + (a_{11}x_{4}^{2}) + (a_{12}x_{1}x_{4})$$

$$y_{3} = a_{13} + (a_{14}x_{2}) + (a_{15}x_{3}) + (a_{16}x_{2}^{2}) + (a_{17}x_{3}^{2}) + (a_{18}x_{2}x_{3})$$

$$y_{4} = a_{19} + (a_{20}y_{1}) + (a_{21}x_{5}) + (a_{22}y_{1}^{2}) + (a_{23}x_{5}^{2}) + (a_{24}y_{1}x_{5})$$

$$y_{5} = a_{25} + (a_{26}y_{2}) + (a_{27}y_{3}) + (a_{28}y_{2}^{2}) + (a_{29}y_{3}^{2}) + (a_{30}y_{2}y_{3})$$

$$y_{6} = a_{31} + (a_{32}y_{4}) + (a_{33}y_{5}) + (a_{34}y_{4}^{2}) + (a_{35}y_{5}^{2}) + (a_{36}y_{4}y_{5})$$

$$(13)$$

#### 5.2. Correlation B (viscosity at the bubble point)

$$\begin{split} y_1 &= a_1 + (a_2 x_2) + (a_3 x_5) + (a_4 x_2^2) + (a_5 x_5^2) + (a_6 x_2 x_5) \\ y_2 &= a_7 + (a_8 x_3) + (a_9 x_5) + (a_{10} x_3^2) + (a_{11} x_5^2) + (a_{12} x_3 x_5) \\ y_3 &= a_{13} + (a_{14} x_2) + (a_{15} x_4) + (a_{16} x_2^2)) + (a_{17} x_4^2) + (a_{18} x_2 x_4) \\ y_4 &= a_{19} + (a_{20} x_1) + (a_{21} x_4) + (a_{22} x_1^2) + (a_{23} x_4^2) + (a_{24} x_1 x_4) \\ y_5 &= a_{25} + (a_{26} y_1) + (a_{27} y_2) + (a_{28} y_1^2) + (a_{29} y_2^2) + (a_{30} y_1 y_2) \\ y_6 &= a_{31} + (a_{32} y_3) + (a_{33} y_4) + (a_{34} y_3^2) + (a_{35} y_4^2) + (a_{36} y_3 y_4) \\ y_7 &= a_{37} + (a_{38} y_5) + (a_{39} y_6) + (a_{40} y_5^2) + (a_{41} y_6^2) + (a_{42} y_5 y_6) \end{split} \tag{14}$$

#### 5.3. Correlation C (viscosity above the bubble point)

```
a_1 = 0.000310658574963
                                                          a_{25} = 0.043019149927751
                             a_{13} = 1.442113843114434
a_2 = -0.000981246034527
                            a_{14} = -0.000808250406804
                                                         a_{26} = 0.160705017685681
a_3 = 0.034005835970458
                            a_{15} = 1.325460888022515
                                                          a_{27} = 0.001077567307166
a_4 = 0.000000102976463
                            a_{16} = 0.000002201405107
                                                          a_{28} = 0.487102977770925
a_5 = -0.000089197699499
                             a_{17} = \ 1.219428706124075
                                                          a_{29} = -0.000000537410482
a_6 = -0.000000144310595
                            a_{18} = -0.005205629557690
                                                          a_{30} = -0.000440674397776
a_7 = 0.000436356306926
                                                          a_{31} = -0.053230296206319
                             a_{19} = 0.523706291515310
a_8 = 0.045829495958338
                             a_{20} = -0.145808969188804 \quad a_{32} = 0.116728945391372
a_9 = -0.006663856121786
                            a_{21} = 0.048747477033081
                                                         a_{33} = 1.033591347286540
                            a_{22} = 0.069361133770155 \\
                                                          a_{34} = -0.525719401610591
a_{10} = -0.000127544730546
a_{11} = 0.000002788372711
                             a_{23} = 0.558113614915075
                                                          a_{35} = -1.227412545950404
                            a_{24} = -0.214773533377629 a_{36} = 1.689369636278221
a_{12} = 0.000001200366564
```

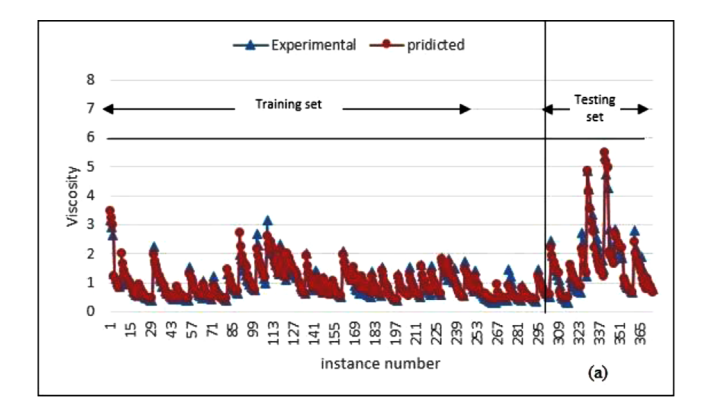
$$\begin{split} y_1 &= a_1 + (a_2 x_1) + (a_3 x_2) + (a_4 x_1^2) + (a_5 x_2^2) + (a_6 x_1 x_2) \\ y_2 &= a_7 + (a_8 x_2) + (a_9 x_3) + (a_{10} x_2^2) + (a_{11} x_3^2) + (a_{12} x_2 x_3) \\ y_3 &= a_{13} + (a_{14} x_3) + (a_{15} x_5) + (a_{16} x_3^2)) + (a_{17} x_5^2) + (a_{18} x_3 x_5) \\ y_4 &= a_{19} + (a_{20} y_1) + (a_{21} y_2) + (a_{22} y_1^2) + (a_{23} y_2^2) + (a_{24} y_1 y_2) \\ y_5 &= a_{25} + (a_{26} y_3) + (a_{27} x_3) + (a_{28} y_3^2) + (a_{29} x_3^2) + (a_{30} y_3 x_3) \\ y_6 &= a_{31} + (a_{32} y_4) + (a_{33} y_5) + (a_{34} y_4^2) + (a_{35} y_5^2) + (a_{36} y_4 y_5) \end{split} \tag{15}$$

where  $x_1$  to  $x_5$  are five input variables consisting oil API gravity, reservoir temperature, solution gas–oil ratio, pressure and saturation pressure, respectively. Besides,  $y_1$  to  $y_6$  are quadratic description of their correspond neurons in Fig. 4.

#### 6. Results and discussion

In this section, correlations results of viscosity below, at, and above the bubble points are discussed through using proposed approach in Fig. 3. The result of correlations and other previous correlations that are tested using the available data are shown in Table 3. The values of MAE, ME, S, and R are achieved by the equations in Appendix A. Relationship between two variables can be measured by correlation coefficient, and unity is the best value that can be gained for the variable. The correlation coefficient of the study is almost equal to 1 as tabulated in Table 3. It can be concluded that there is a remarkable difference between correlation coefficient of this study and the previous ones. The proposed correlations also provide better results in comparison with the other correlations, which are evaluated in the study.

The divergence between obtained outputs of the presented model and corresponding experimental data are presented in Figs. 5 and 6. The obtained results of the presented model for



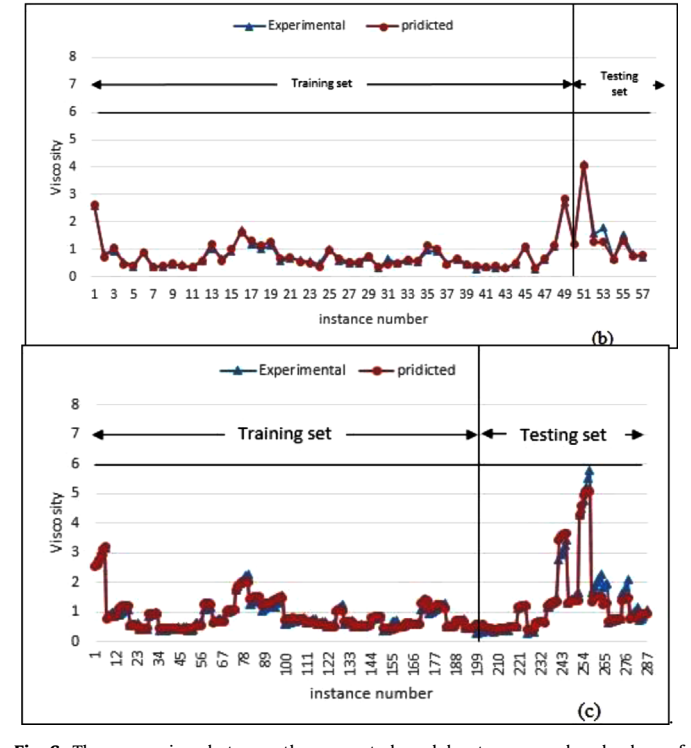


**Fig. 6.** The comparison between the presented model outcomes and real values of viscosity at bubble point. (a) Viscosity below the bubble point. (b) Viscosity at the bubble point. (c) Viscosity above the bubble point.

viscosity below, at and above the bubble points is according to the line Y=X, representing good precision. Correlation coefficient  $(R^2)$  of the above-mentioned line represents the strength of the model. The best value that can be obtained for this variable is equal to 1. Fig. 6 depicts training and testing datasets for predicting of Iranian crude oils viscosity. Not only does this GS-GMDH model, combined by genetic algorithm, have brilliant behavior, but the model in terms of simple polynomial equations are able to model and forecast properly the output of testing data that are not employed throughout the training process as well.

Relative deviation of the obtained output values of presented model using experimental values is illustrated in Fig. 7. In addition, relative deviations of the determined viscosity values by presented model in terms of pressure values is depicted in Fig. 8. Figs. 7 and 8 can show performance of the evolved presented model.

The comparison between the correlation coefficient of the presented model and the seven aforementioned models are illustrated in Fig. 9. Since there is considerable difference between the correlations values of presented model and the seven others studies, according to Fig. 9 it would not be wrong to come to the conclusion that presented model has superiority over the other

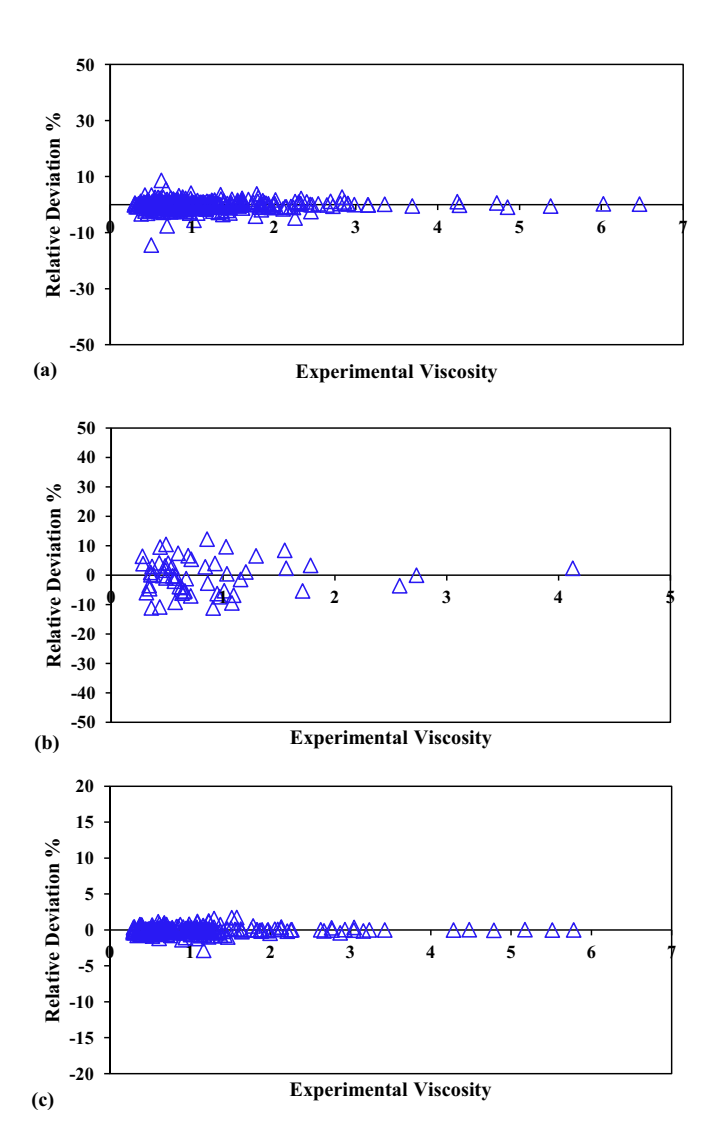


**Fig. 7.** Relative deviations of the determined viscosity values by presented model using experimental values. (a) Viscosity below the bubble point. (b) Viscosity at the bubble point. (c) Viscosity above the bubble point.

discussed models for estimating and predicting of the viscosity of Iranian crude oils.

Sensitivity analysis also is carried out to determine the influence of oil API gravity and pressure on the viscosity below the bubble point. The viscosity data are plotted in terms of reservoir temperature in Figs. 10 and 11 with respect to pressure and oil API gravity. Constant temperatures are depicted by the similar color. Fig. 10 illustrates that the slop of viscosity in terms of pressure (0–6000 psi) is first increased isothermally and linearly, and it is then reduced. Fig. 11 shows that the values of viscosity in terms of oil API gravity is first linearly increased for different constant temperature, and it is then declined.

#### 7. Conclusion

In this paper, a multi-hybrid model is employed to predict the viscosity of Iranian crude oils. The viscosity correlations are obtained for each below, at, and above bubble points. These correlations are trained and tested by a data set with a wide range of input parameters. Genetic algorithm is then employed to generate new data stochastically and the new data then enter to the GS-

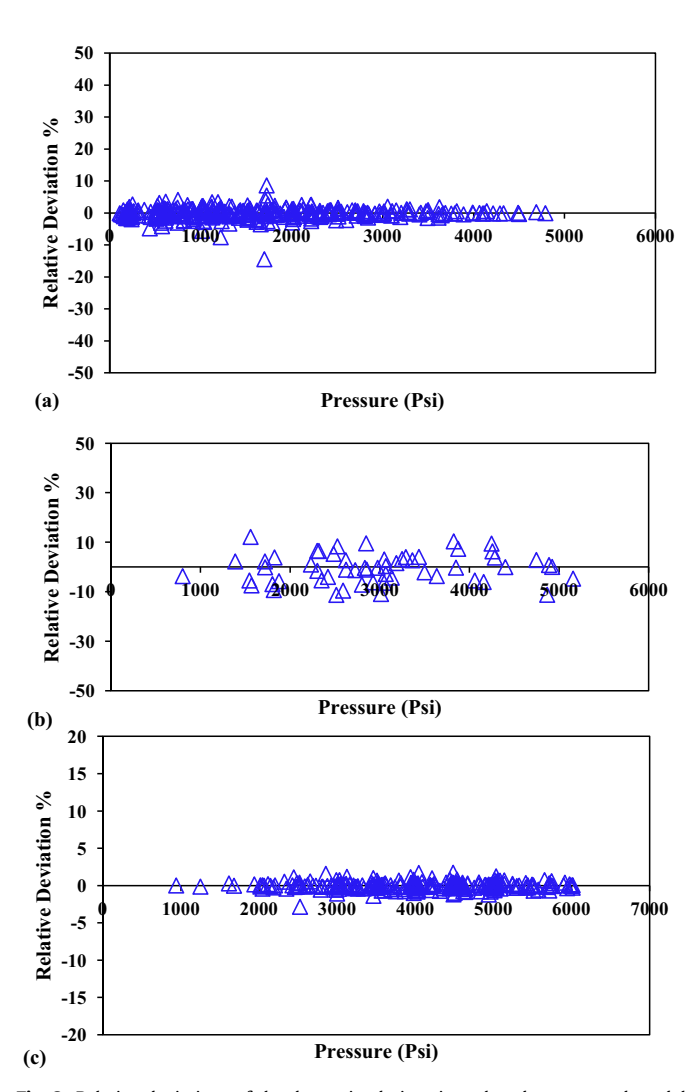


**Fig. 8.** Relative deviations of the determined viscosity values by presented model in terms of pressure values. (a) Viscosity below the bubble point. (b) Viscosity at the bubble point. (c) Viscosity above the bubble point.

GMDH model. This process is occurred in the range of decision variables. The proposed multi-hybrid-model has presented ideal correlation. The obtained correlations coefficient are about 0.9996, 0.9944, and 0.9999 for below, at, and above the bubble points, respectively. In addition, the accuracy of proposed model is compared to seven well-known models. Results show that the proposed multi-hybrid model has considerable superiority over the other models for estimating the viscosity of Iranian crude oils. This paper can trigger further implications to predict oil physiochemical properties more appropriately.

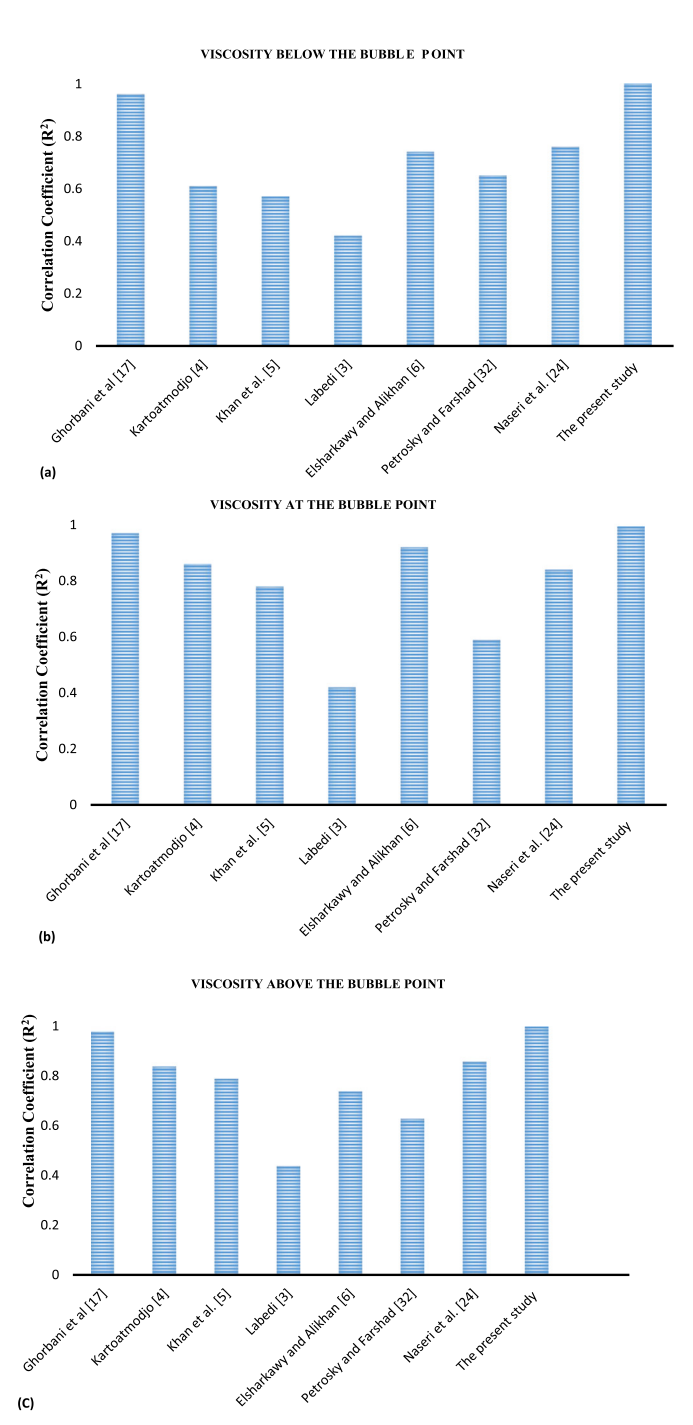


**Fig. 9.** Comparison between obtained correlation in different studies and presented study. (a) Viscosity below the bubble point. (b) Viscosity at the bubble point. (c) Viscosity above the bubble point.

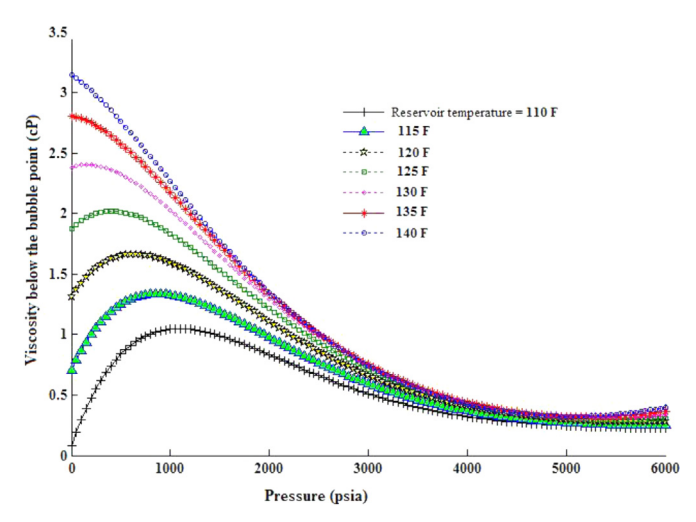


Fig. 10. Deviation of viscosity below the bubble point vs. pressure.

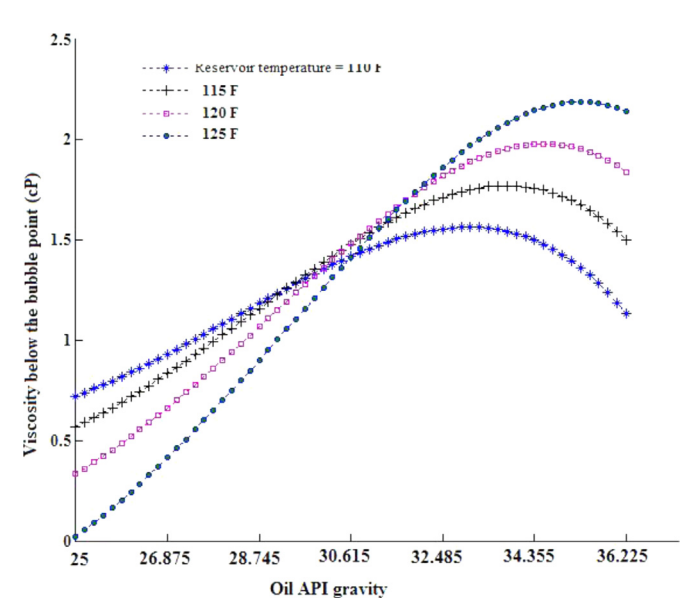


Fig. 11. Deviation of viscosity below the bubble point vs. oil API gravity.

#### Appendix A. Statistical analysis

1. Percent relative error

$$E_i = \left(\frac{X_{\text{exp}} - X_{\text{est}}}{X_{\text{exp}}}\right)_i \times 100 \ (i = 1, 2, ..., n)$$

2. Percent mean relative error

$$E_r = \frac{1}{n} \sum_{i=1}^n E_i$$

3. Percent mean absolute relative error

$$E_a = \frac{1}{n} \sum_{i=1}^n |E_i|$$

4. Standard deviation

$$S = \sqrt{\frac{1}{n-1} \sum_{i=1}^{n} \left( E_i - E_r \right)^2}$$

5. The correlation coefficient

$$r = \sqrt{1 - \sum_{i=1}^{n} [X_{\text{exp}} - X_{\text{est}}]_{i}^{2} / \sum_{i=1}^{n} [X_{\text{exp}} - \overline{X}]_{i}^{2}}$$

where

$$\overline{X} = \frac{1}{n} \sum_{i=1}^{n} [X_{\exp}]_i$$

#### References

Abedini, R., Abedini, A., Yakhfrouzan, N.E., 2010. A new correlation for prediction of undersaturated crude oil viscosity. Pet. Coal 52 (1), 50–55.

Ahmadi, M.A., 2015. Connectionist approach estimates gas—oil relative permeability in petroleum reservoirs: application to reservoir simulation. Fuel 140, 429–439.

Ahmadi, M.H., Ahmadi, M.-A., Mehrpooya, M., Rosen, M.A., 2015. Using GMDH neural networks to model the power and torque of a stirling engine. Sustainability 7 (2), 2243–2255.

Al-Marhoun, M., Nizamuddin, S., Raheem, A.A., Ali, S.S., Muhammadain, A., 2012. Prediction of crude oil viscosity curve using artificial intelligence techniques. J. Pet. Sci. Eng. 86, 111–117.

Amidpour, M., Hamedi, M., Mafi, M., Ghorbani, B., Shirmohammadi, R., Salimi, M., 2015. Sensitivity analysis, economic optimization, and configuration design of mixed refrigerant cycles by NLP techniques. J. Nat. Gas Sci. Eng. 24, 144–155.

Ardalan, H., Eslami, A., Nariman-Zadeh, N., 2009. Piles shaft capacity from CPT and CPTu data by polynomial neural networks and genetic algorithms. Comput. Geotech. 36 (4), 616–625.

Elsharkawy, A., Alikhan, A., 1999. Models for predicting the viscosity of Middle East crude oils. Fuel 78 (8), 891–903.

Ghaderi, A., 2012. New predictive tools to estimate diesel oil density and viscosity. J. Pet. Sci. Eng. 98, 19–21.

Ghorbani, B., Mafi, M., Shirmohammadi, R., Hamedi, M.-H., Amidpour, M., 2014. Optimization of operation parameters of refrigeration cycle using particle swarm and NLP techniques. J. Nat. Gas Sci. Eng. 21, 779–790.

Ghorbani, B., Ziabasharhagh, M., Amidpour, M., 2014. A hybrid artificial neural network and genetic algorithm for predicting viscosity of Iranian crude oils. J. Nat. Gas Sci. Eng. 18. 312–323.

Glaso, O., 1980. Generalized pressure–volume–temperature correlations. J. Pet. Technol. 32 (05), 785–795.

Hajizadeh, Y., 2007a. Intelligent prediction of reservoir fluid viscosity. Paper presented at the Production and Operations Symposium.

Hajizadeh, y., 2007b. Viscosity prediction of crude oils with genetic algorithms. Paper presented at the Latin American Caribbean Petroleum Engineering Conference.

Hemmati-Sarapardeh, A., Khishvand, M., Naseri, A., Mohammadi, A.H., 2013. To-ward reservoir oil viscosity correlation. Chem. Eng. Sci. 90, 53–68.

Hou, J., Li, X., Sui, H., 2015. The optimization and prediction of properties for crude oil blending. Comput. Chem. Eng. 76, 21–26.

Kartoatmodjo, T., Schmidt, Z., 1994. Large data bank improves crude physical property correlations. Oil Gas J. 92 (27).

Khan, S., Al-Marhoun, M., Duffuaa, S., Abu-Khamsin, S., 1987. Viscosity correlations for Saudi Arabian crude oils. Paper presented at the Middle East Oil Show.

Labedi, R., 1992. Improved correlations for predicting the viscosity of light crudes. J. Pet. Sci. Eng. 8 (3), 221–234.

Madandoust, R., Ghavidel, R., Nariman-Zadeh, N., 2010. Evolutionary design of generalized GMDH-type neural network for prediction of concrete compressive strength using UPV. Comput. Mater. Sci. 49 (3), 556–567.

Makinde, F., Ako, C., Orodu, O., Asuquo, I., 2012. Prediction of crude oil viscosity using feed-forward back-propagation neural network (FFBPNN). Pet. Coal 54 (2), 120–131.

Nariman-Zadeh, N., Darvizeh, A., Ahmad-Zadeh, G., 2003. Hybrid genetic design of GMDH-type neural networks using singular value decomposition for modelling and prediction of the explosive cutting process. Proc. Inst. Mech. Eng. B: J. Eng. Manuf. 217 (6), 779–790.

Nariman-Zadeh, N., Darvizeh, A., Jamali, A., Moeini, A., 2005. Evolutionary design of generalized polynomial neural networks for modelling and prediction of explosive forming process. J. Mater. Process. Technol. 164, 1561–1571.

Naseri, A., Nikazar, M., Dehghani, S.M., 2005. A correlation approach for prediction of crude oil viscosities. J. Pet. Sci. Eng. 47 (3), 163–174.

Park, J.H., Khan, M.S., Lee, M., 2014. Modified coordinate descent methodology for solving process design optimization problems: application to natural gas plant. J. Nat. Gas Sci. Eng.

Petrosky, Jr, G., Farshad, F. Viscosity correlations for Gulf of Mexico crude oils. in: SPE Production Operations Symposium, 1995. Society of Petroleum Engineers.

Shirmohammadi, R., Ghorbani, B., Hamedi, M., Hamedi, M.-H., Romeo, L.M., 2015. Optimization of mixed refrigerant systems in low temperature applications by means of group method of data handling (GMDH). J. Nat. Gas Sci. Eng. 26, 303–312.

Torabi, F., Abedini, A., Abedini, R., 2011. The development of an artificial neural network model for prediction of crude oil viscosities. Pet. Sci. Technol. 29 (8): 804–816.

Wang, J., Dong, M., 2009. Optimum effective viscosity of polymer solution for improving heavy oil recovery. J. Pet. Sci. Eng. 67 (3), 155–158.